



Theoretical characterization of intermolecular vibrational states through the multi-configuration time dependent Hartree approach: The He₂,3ICI clusters

Álvaro Valdés, Rita Prosimiti, Pablo Villarreal, and Gerardo Delgado-Barrio

Citation: *J. Chem. Phys.* **135**, 244309 (2011); doi: 10.1063/1.3671611

View online: <http://dx.doi.org/10.1063/1.3671611>

View Table of Contents: <http://jcp.aip.org/resource/1/JCPSA6/v135/i24>

Published by the [American Institute of Physics](http://www.aip.org).

Additional information on *J. Chem. Phys.*

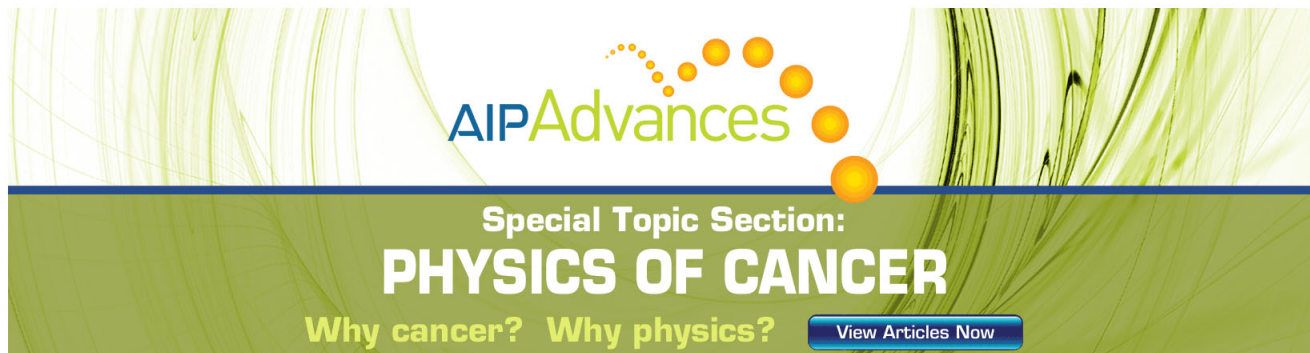
Journal Homepage: <http://jcp.aip.org/>

Journal Information: http://jcp.aip.org/about/about_the_journal

Top downloads: http://jcp.aip.org/features/most_downloaded

Information for Authors: <http://jcp.aip.org/authors>

ADVERTISEMENT



AIPAdvances

Special Topic Section:
PHYSICS OF CANCER

Why cancer? Why physics? [View Articles Now](#)

Theoretical characterization of intermolecular vibrational states through the multi-configuration time dependent Hartree approach: The $\text{He}_{2,3}\text{ICl}$ clusters

Álvaro Valdés,^{a)} Rita Prosmi, Pablo Villarreal, and Gerardo Delgado-Barrio
Instituto de Física Fundamental (IFF-CSIC), CSIC, Serrano 123, 28006 Madrid, Spain

(Received 2 November 2011; accepted 1 December 2011; published online 28 December 2011)

Benchmark, full-dimensional calculations on the ground and excited vibrational states for the tetra-, and penta-atomic weakly bound $\text{He}_{2,3}\text{ICl}$ complexes are reported. The representation of the potential energy surfaces includes three-body HeICl potentials parameterized to coupled-cluster singles, doubles, and perturbative triples *ab initio* data. These terms are important in accurately describing the interactions of such highly floppy systems. The corresponding 6D/9D computations are performed with the multi-configuration time dependent Hartree method, using natural potential fits, and a mode combination scheme to optimize the computational effort in the improved relaxation calculations. For these complexes several low-lying vibrational states are computed, and their binding energies and radial/angular probability density distributions are obtained. We found various isomers which are assigned to different structural models related with combinations of the triatomic isomers, like linear, T-shaped, and antilinear ones. Comparison of these results with recent experimental data is presented, and the quantitative deviations found with respect to the experiment are discussed. © 2011 American Institute of Physics. [doi:10.1063/1.3671611]

I. INTRODUCTION

The development of experimental techniques, such as supersonic nozzle expansion,^{1–9} and the advantages of *ab initio* electronic structure calculations^{10–15} and quantum-mechanical methods,^{16–21} has made possible to study the structure and dynamics of weakly bound systems in more detail. The present work is directed at investigating the aspects of the multidimensional potential energy surfaces (PES) of van der Waals (vdW) complexes, e.g., formed by a few He atoms and the heteronuclear ICl dihalogen molecule, and their effect on spectroscopic features. This work forms part of an extended investigation of such prototypical interactions and, in particular for the He_NICl case with $N = 1, 2,$ and $3,$ permits a direct comparison between first principles computations and the available experimental data.^{22–24} To our knowledge, there are no previous full dimensional theoretical studies dealing with the tetra- and penta-atomic species of this series, while experimental data have been recently reported.²² Laser-induced fluorescence (LIF) and two-color action spectroscopy techniques have been utilized to record discrete features associated with transitions of multiple conformers of the $\text{He}_{2,3}\text{Br}_2$ and $\text{He}_{2,3}\text{ICl}$ complexes, with the energetic ordering of them in agreement with previous theoretical predictions on the tetra-atomic species.^{21,25} In these earlier studies variational calculations with reduced dimensionality have been reported using PESs which are based on the sum of three-body interactions for these systems.^{21,25–27} Also, for larger complexes quantum-chemistry-like treatments have been reported,^{28–30} and in case of the He_NICl clusters with $3 < N < 30$ such calculations have been also carried out using

the same multi-body surface to simulate the spectra of polar molecules embedded in ^4He environment.³¹

Recently, we showed that for $\text{He}_{2,3}\text{Br}_2$ complexes the multi-configuration time-dependent Hartree (MCTDH) method^{32,33} can be efficiently used to provide the energies and structural properties of different isomers.³⁴ Thus, this methodology is employed now to describe the $\text{He}_{2,3}\text{ICl}$ complexes, which present higher anisotropy, as compared to the case with a homonuclear dopant, $\text{He}_{2,3}\text{Br}_2$. In particular, for the triatomic HeICl cluster earlier coupled-cluster single double triple (CCSD(T)) calculations have predicted the existence of three potential minima, with decreasing well-depths values from linear to near T-shaped to antilinear configurations. This topology of the potential was found to mark clearly the HeICl measured spectra as well as the complexes of higher order,^{22,24} and it is expected to have a persistent effect on our present computations. As the number of degrees of freedom increases the exact calculation of intermolecular vibrational states becomes more laborious, and even computationally prohibitive for the traditional variational methods. For larger clusters approximate methods are then employed to handle the computational effort, and insights on anharmonic quantum effects for smaller species become useful in guiding them. Therefore, such benchmark results are desirable for both resolving issues on the PES representation, and serving as a quantitative check of new or approximate approaches.

The paper is organized as follows. In Sec. II we describe some computational and methodological details of the *ab initio* calculations used for the potential representation and the MCTDH computations of the He_NICl , $N = 1, 2, 3,$ vibrational states. The results of these calculations are also presented. In particular, the characterization of different conformers and the spectroscopic properties of some of them

^{a)}Electronic mail: alvaro.v@iff.csic.es.

are discussed in comparison with the available experimental data. Besides, few vibrational excited states corresponding to He–He stretching modes in the T-shaped well arrangements configurations are also calculated for $N = 2$ and 3 complexes. Section III contains some concluding remarks.

II. COMPUTATIONS, RESULTS, AND DISCUSSION

The methodology used to compute the bound states of the He_NICl systems has been recently detailed in Ref. 34. The molecular Hamiltonian is described in satellite coordinates (\mathbf{r} , \mathbf{R}_k), \mathbf{r} is the vector joining the I and Cl atoms and \mathbf{R}_k are the vectors from the center of mass of the I–Cl molecule to the $k = 1, \dots, N$ He atoms. The Hamiltonian takes the form

$$\hat{H} = -\frac{\hbar^2}{2m} \frac{\partial^2}{\partial r^2} + \frac{\mathbf{j}^2}{2mr^2} + \sum_{k=1}^N \left(-\frac{\hbar^2}{2\mu} \frac{\partial^2}{\partial R_k^2} + \frac{\mathbf{l}_k^2}{2\mu R_k^2} \right) - \frac{\hbar^2}{m_{\text{ICl}}} \sum_{k<l} \nabla_k \cdot \nabla_l + V(\mathbf{r}, \mathbf{R}_1, \dots, \mathbf{R}_N), \quad (1)$$

where \mathbf{j} and \mathbf{l}_k are the angular momenta associated to the vectors \mathbf{r} and \mathbf{R}_k , respectively. m is the reduced mass of the diatomic ICl molecule, μ is the reduced mass of the He–ICl system and m_{ICl} is the sum of the masses of the I and Cl atoms. The effect of the kinetic energy coupling terms ($-\hbar^2/m_{\text{ICl}} \sum_{k<l} \nabla_k \cdot \nabla_l$) has been estimated to be less than 0.02 cm^{-1} in the energy of the states from five dimensional (5D) variational calculations for both He_2Br_2 and the He_2ICl molecules,^{16,21,25} and thus we did not consider this term further on.

A. *Ab initio* calculations and potential form

For the He_2XY , $\text{XY} = \text{Br}_2, \text{ICl}$, tetra-atomic molecules it has been shown that a potential form consisting in the sum of the three-body HeICl interactions plus the He–He interaction is able to describe very accurately the 5D tetra-atomic *ab initio* CCSD(T) potential.^{21,25} Recently, work on He_3Br_2 showed that the extension of this potential form to penta-atomic molecules together with the capabilities of the MCTDH method to describe systems with high dimensionality can provide a very detailed description of its lowest vibrational states in agreement with the experimental findings.^{22,34} In this work we use again such representation to describe the $\text{He}_N\text{–ICl}$, $N=1, 2, 3$, molecules, with the potential form being

$$V(\mathbf{r}, \mathbf{R}_1, \dots, \mathbf{R}_N) = \sum_k V_{\text{HeICl}}(\mathbf{r}, \mathbf{R}_k) + \sum_{k<l} V_{\text{He–He}}(\mathbf{R}_k, \mathbf{R}_l) + U_{\text{ICl}}(\mathbf{r}), \quad (2)$$

where the $V_{\text{HeICl}}(\mathbf{r}, \mathbf{R}_k)$ terms are the CCSD(T) parameterized potential of the HeICl complex described below, the $V_{\text{He–He}}(\mathbf{R}_k, \mathbf{R}_l)$ terms are the potential function for He_2 given in Ref. 35, and $U_{\text{ICl}}(\mathbf{r})$ is the diatomic interaction ICl potential calculated at the CCSD(T) level of theory, as the triatomic one, and is given in the supplementary material (see Table I).³⁶

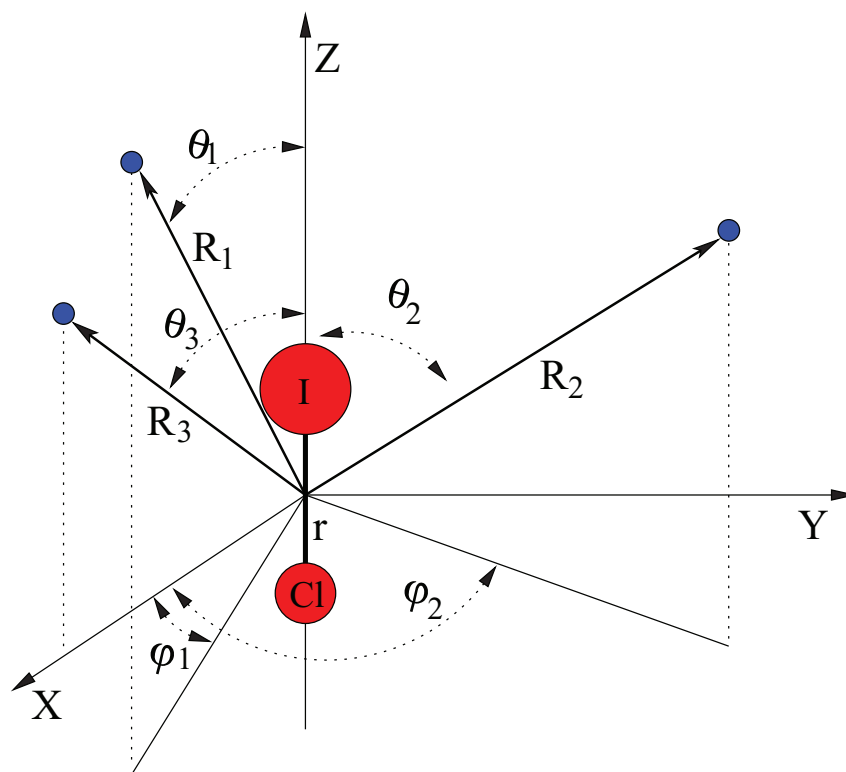
TABLE I. Well-depths (D_e in cm^{-1}) and equilibrium distances (R_e in angstroms and φ_i^e in degrees) for the indicated (#T,#L,#A) configurations of the He_NICl systems, with $N = 1, 2, 3$ and $r_e = 2.321 \text{ \AA}$.

(#T,#L,#A)	D_e	R_e^e	φ_i^e
(0,1,0)	–58.62	3.86	...
(1,0,0)	–38.97	3.81	...
(0,0,1)	–38.03	5.12	...
(1,1,0)	–97.72	3.82/3.86	...
(0,1,1)	–96.67	3.85/5.12	...
(2,0,0)	–85.64	3.81	48.80
(1,0,1)	–77.40	3.82/5.12	...
(2,1,0)	–144.51	3.86/3.81/3.81	0.00/48.80
(1,1,1)	–136.16	3.86/3.81/5.12	...
(3,0,0)	–132.63	3.81/3.81/3.81	48.90/97.55

We used the sets of (r, R_3, θ_3) , $(r, R_1, R_3, \theta_1, \theta_3, \varphi_1)$, and $(r, R_1, R_2, R_3, \theta_1, \theta_2, \theta_3, \varphi_1, \varphi_2)$ coordinates shown in Fig. 1, to describe the HeICl, He_2ICl , and He_3ICl systems, respectively. *Ab initio* computations of the HeICl interaction at fixed ICl bond distances of $r = 2.271, 2.321$, and 2.386 \AA have been reported at the CCSD(T) level of theory.^{31,37} To account for the dependence on r we extend here these calculations in two more values of r , 2.15, and 2.5 \AA , in order to describe the whole range of the $v = 0$ and 1 vibrational states of ground state ICl molecule. Following the fitting procedure of Ref. 37 the 3D PES is described by a Morse+vdW analytical function in R_3 and θ_3 coordinates, while for the r a 1D cubic-spline interpolation is employed. The potential parameters for $r = 2.15$ and 2.5 \AA are listed in the supplementary material (see Table II),³⁶ while for the other three values of r they are given in Tables II and III of Refs. 31 and 37, respectively. The model potential reproduces very well the *ab initio* triatomic values with maximum standard deviation of 0.94 cm^{-1} , and an average standard deviation of 0.14 cm^{-1} for all previous and present (r, R_3, θ_3) values.

In the case of heteronuclear dihalogen molecules, it has been found that the PESs of rare gas-dihalogen complexes support a triple-minima topology, corresponding to linear, near T-shaped and antilinear configurations for their electronic ground states.^{4,12,26,37} In particular for the HeICl potential in the r range studied, the global minimum with an energy of -58.62 cm^{-1} at $R_3 = 3.86 \text{ \AA}$ and $r = 2.321 \text{ \AA}$ corresponds to a linear He–I–Cl ($\theta_3 = 0^\circ$) configuration. The second minimum, with energy of -42.75 cm^{-1} , is at $R_3 = 3.75 \text{ \AA}$ and $r = 2.15 \text{ \AA}$ corresponding to a near T-shaped ($\theta_3 = 110.9^\circ$) configuration of the complex, while the last one is found for antilinear He–Cl–I ($\theta_3 = 180^\circ$) geometry at energy of -38.032 cm^{-1} at $R_3 = 5.12 \text{ \AA}$ and $r = 2.321 \text{ \AA}$. We label the different equilibrium geometries as (#T,#L,#A), where #T, #L and #A are the number of He atoms in the near T-shaped, linear, and antilinear geometries, respectively.

In Table I the well-depths and equilibrium geometries for the HeICl, He_2ICl , and He_3ICl complexes are given at the equilibrium ICl distance, r_e . For the tetra-atomic system four minima on the surface are reported here in complete accord with the ones found previously in Ref. 37, while for

FIG. 1. Schematic representation of coordinate system for He₃ICl complex (see text).

the penta-atomic cluster we present only three optimal structures, which are related with the triatomic and tetra-atomic complexes mentioned above. These are found at energies of -144.51 , -136.16 , and -132.63 cm^{-1} corresponding to the (2,1,0), (1,1,1), and (3,0,0) configurations, respectively. In Fig. 2 we show 2D contour plots for the He₃ICl surface in the Cartesian (Z,X) and (X,Y) planes. The ICl molecule is frozen along the Z-axis in its equilibrium geometry ($r_e = 2.321$ Å), with the two He atoms being also fixed at their tetra-atomic equilibrium positions of Table I, while the remaining He atom is allowed to move in the (Z,X) or (X,Y) plane. The tetra-atomic molecule is fixed to a (0,1,1) configuration in panel

of Fig. 2(a), (1,1,0) configuration in panels of Figs. 2(b) and 2(c) and (2,0,0) configuration in panel of Fig. 2(d). One can see that several stationary points of the surface are shown in these plots, corresponding to bending configurations of the He atoms, like the ones in Figs. 2(a) and 2(b) at angle values of around 40° and 140° , which are related with the “bifork” structures found previously for the tetra-atomic He₂ICl.³⁷

In order to evaluate the quality of the analytical expression of the Eq. (2), we performed CCSD(T) electronic structure calculations^{38,39} at the above mentioned optimal configurations for each of the three complexes. We employed both large- and small core ECPs, ECP46MWB, and

TABLE II. Potential values and interaction energies for the indicated configurations of He_NICl (N = 1, 2, and 3), and their complete basis set limit values at CCSD(T) level of theory, using large- (ECP46MWB) and small-core (ECP28MDF) pseudopotentials together with the SDB-AVT/QZ or AVXZ-PP, X = T,Q,5 basis sets for I and AVXZ for He and Cl atoms, respectively. bf stands for the set (3s3p2d2f1g) of bond functions.³⁷

(#T,#L,#A)	ECP46MWB(SDB-AVT/QZ)	ECP28MDF(AVT/Q/5Z-PP)	CBS[TQ5]	PES Eq. (2)
	AVTZ+bf ^{a,b} /AVQZ ^b /AVQZ	AVTZ/AVQZ/AV5Z		
(0,1,0)	-58.37/-54.72/-60.32	-46.07/-54.39/-57.59	-59.45	-58.63
(1,0,0)	-39.83/-37.23/-38.85	-32.24/-37.11/-39.46	-40.83	-38.97
(0,0,1)	-37.66/-34.80/-35.17	-30.44/-34.63/-36.35	-37.35	-38.03
(1,1,0)	-/-92.10/-99.34	-78.42/-91.64/-97.18	-100.41	-97.72
(0,1,1)	-/-89.40/-95.39	-78.42/-91.64/-97.18	-96.75	-96.67
(2,0,0)	-/-81.74/-85.02	-70.94/-81.46/-86.53	-89.50	-85.64
(2,1,0)	-/-136.78/-145.69	-117.32/-136.17/-144.39	-149.18	-144.51
(1,1,1)	-/-127.34/-134.95	-109.34/-126.71/-133.90	-138.09	-136.16
(3,0,0)	-/-126.51/-131.43	-110.08/-126.09/-133.82	-138.35	-132.63

^aThe basis set used are given in Ref. 37.

^bThese calculations are carried out without core polarization potential corrections (CPP).

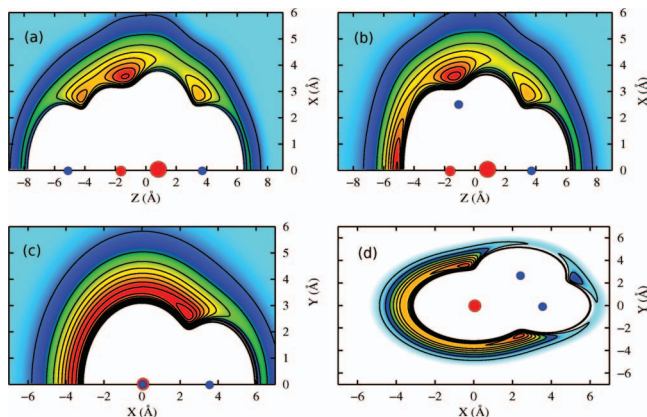


FIG. 2. Contour plots of the He_3ICl potential energy surface, $V(r, R_1, R_2, R_3, \theta_1, \theta_2, \theta_3, \varphi_1, \varphi_2)$ in the ZX (a, b) and XY (c, d) Cartesian planes. The ICl distance is fixed at 2.321 Å along the Z-axis, while the geometry of the tetra-atomic molecule is fixed to a linear (0,1,1) configuration (a), police-nightstick (1,1,0) configuration (b, c), and tetrahedral (2,0,0) configuration (d) with the He atoms in the equilibrium positions of Table I. Contour intervals are of 5 cm^{-1} for energies from 135 cm^{-1} in panel (a), 140 cm^{-1} in panels (b) and (c), and 130 cm^{-1} in panel (d).

ECP28MDF, in conjunction with the SDB-aug-cc-pVTQZ and aug-cc-pVXZ-PP basis sets for the valence electrons of the I atom,^{40–42} while for the He/Cl atoms a series of correlation consistent basis sets is used,⁴³ allowing to obtain interaction energies at the complete basis set, CBS) limit. We used the three-point extrapolation scheme by Peterson *et al.*⁴⁴ with $X = \text{T, Q}$, and 5 the cardinal number of the aug-cc-pVXZ series basis sets. The results of the calculated interaction energies are listed in Table II. As it can be seen for the triatomic case the analytical PES describes pretty well the indicated

configurations compared to the original *ab initio* values using the basis sets from Ref. 37, with differences of no more than 0.9 cm^{-1} , that is similar to the maximum deviation value mentioned above for the fitting procedure. Also comparing the potential values with a more accurate calculation of the interaction energies at the CBS[TQ5] limit (see Table II), we found that the maximum difference counts to 1.9 cm^{-1} , with deeper well depths for (0,1,0) and (1,0,0) configurations, and shallower for the (0,0,1) one. These differences are directly reflected to the corresponding values for the tetra- and penta-atomic species, where the additivity of the interaction forces could be checked at each CCSD(T) calculation. Thus, deviations at the most of ≈ 4 and 6 cm^{-1} are expected for the He_2ICl and He_3ICl potentials, respectively, taken as reference data from the CBS[TQ5] computations.

B. MCTDH calculations

To solve the eigenvalue problem we use the *improved relaxation* method implemented in the Heidelberg MCTDH code.^{32,33,45} The MCTDH program requires the potential energy operator to be written as the sum of products of single-particle operators. The POTFIT program is used to obtain the desired product representation by expanding the PES in natural potentials.^{23,46} In Table III we present the parameters used for the POTFIT calculations, together with the primitive basis employed in both POTFIT and the MCTDH calculations. For each degree of freedom we show the corresponding type of basis set used, where *sin* stands for the sine *discrete variable representation* (DVR) basis, *HO* is for the harmonic oscillator DVR basis and *Leg* and *Pleg* correspond to the one and two dimensional Legendre DVR basis, respectively. The number

TABLE III. POTFIT and MCTDH parameters used in the refitting of the PESs. For each coordinate we list the number and type of primitive basis set, as well as the range covered by the calculations. The number of natural potentials, the relevant regions of the potential together with the root-mean-square error for the fits are also given. Contr stands for the mode over which a contraction is done.

	HeICl(r, R_3, θ_3)	He–He($R_1, R_3, \theta_1, \theta_3, \varphi_1$)	He–He($R_1, R_2, \theta_1, \theta_2, \varphi_1, \varphi_2$)
Primitive basis			
N_r (sin)	35
r-range (Å)	[2.15, 2.50]
N_R (HO)	41	41	41
R-range (Å)	[2.80, 7.41]	[2.80, 7.41]	[2.80, 7.41]
N_θ (Leg) / N_θ (Pleg)	21 / 0	21 / 21	0 / 21
θ -range (rad)	[0, π]	[0, π]	[0, π]
N_φ	...	15	15
φ -range (rad.)	[0, 2π]	[0, 2π]	[0, 2π]
Natural potentials			
N_r	20
N_R	20
N_θ	Contr
$N_{R_1\theta_1/R_2\theta_3}$...	Contr/150	...
$N_{R_1\theta_1/R_2\theta_2}$	Contr/150
N_{φ_1/φ_2}	...	10/-	10/10
Relevant regions	$V < 20 \text{ cm}^{-1}$	$V < 5 \text{ cm}^{-1}$	$V < 5 \text{ cm}^{-1}$
rms error on relevant grid points (cm^{-1})	$< 10^{-3}$	0.1	0.4

TABLE IV. Number of single-particle functions (SPF) and least populated orbital population of the MCTDH *improved relaxation* calculations.

	HeICI	He ₂ ICI	He ₃ ICI
SPF			
N _r	3	2	1
N _{R₃}	10
N _{R₁,θ₁}	...	12	5
N _{R₂,θ₂}	5
N _{R₃,θ₃}	...	12	5
N _{φ₁}	...	5	...
N _{φ₁φ₂}	12
Least populated orbital population	1 × 10 ⁻⁷	1 × 10 ⁻⁵	5 × 10 ⁻⁵

of natural potentials included in the POTFIT calculations for the V_{HeICI} and V_{He-He} potential energy surfaces are also listed. As φ₃ is set to 0 (see Fig. 1), different fittings (5D and 6D) of the V_{He-He} potential are performed in the penta-atomic case to consider all the He-He interactions. The introduction of weights can increase the accuracy of the potential fit for the relevant regions, and thus in Table III we list the relevant regions of the potential considered in the above mentioned calculations, as well as the root mean square (rms) error for all the fits.

The Hamiltonian operators employed here, for zero total angular momentum in the coordinates described in Fig. 1, for N = 1, 2, and 3 has been previously presented in Refs. 14, 17, and 34, respectively. The parity under R_i ↔ R_j exchange is not taken into account in the present calculations. In Table IV we resume the number of single particle functions (SPFs) included in the *improved relaxation* calculations for He_NICI with N = 1, 2, 3. By taking advantage of the nature of these He complexes in which a helium atom is barely affected by the other ones, we introduce here a mode combination scheme that differs from the one used previously.³⁴ The correlation of the R_i and θ_i, for i running on the different He atoms, is very strong, and we show that the contraction of these degrees of freedom into one mode speeds up the calculations significantly. Moreover, this scheme allows the construction of very convenient initial wavefunctions by considering for each contracted mode (R_i,θ_i) the eigenfunction corresponding to the solutions of the HeICI 2D problem. For the r coordinate of the ICI distance one SPF function is enough to describe the lowest vdW states. The population of a second SPF on this degree of freedom was found to be of less than 10⁻⁵ for *improved relaxation* calculations of the ground vdW states of the He₂ICI and He₃ICI complexes. The populations of the highest (least populated) natural orbital of the other modes is included for the three cases in Table IV. The improved relaxation runs are converged to within 10⁻⁴ cm⁻¹.

C. Vibrational bound states

The results of the bound state calculations are summarized in Table V. We also label the computed states as (#T,#L,#A)^{v=i} following the notation mentioned above, to characterize the averaged vibrational structure of the

TABLE V. Zero point energies (ZPE) and their % values (in parenthesis) of the corresponding potential well-depths (see Table I), together with the binding energies (D₀) for the different He_NICI isomers, with N = 1, 2, 3. The comparison with experimental observations (Ref. 24) and previous theoretical results is also included. Energies are in cm⁻¹.

(#T,#L,#A)	ZPE(%)		D ₀	
	This work		Theor.	Expt.
(0,1,0)	40.23(68.6%)	18.390	18.29 (2D) ^a	22.0(2)
(1,0,0)	23.83(61.2%)	15.137	15.15 (2D) ^a	16.6(3)
(0,0,1)	25.73(67.7%)	12.298	12.33 (2D) ^a	
(1,1,0) (5D/6D)	64.03(65.5%)	33.664/33.692	33.514 ^b /-	38.6(4)
(0,1,1) (5D/6D)	65.79(68.0%)	30.818/30.883	31.598 ^b /-	
(2,0,0) (5D/6D)	54.82(64.0%)	30.925/30.820	30.465 ^b /-	33.2(4)
(2,0,0) ^{v=1} (5D/6D)	...	29.804/29.730	29.191 ^b /-	
(2,0,0) ^{v=2} (5D/6D)	...	28.513/29.505	-/-	
(1,0,1) (5D/6D)	49.23(63.6%)	28.184/28.167	28.033 ^b /-	
(2,1,0)	94.91(65.7%)	49.599
(2,1,0) ^{v=1}	...	48.418
(3,0,0)	85.36(64.4%)	47.273
(3,0,0) ^{v=1}	...	45.728
(1,1,1)	89.32(65.6%)	46.838

^aReference 37.

^bReference 21

molecule, and a super-index $v = i$ is added to indicate that the referred state is i times vibrationally excited in the He-He stretching mode. The calculated binding energies and zero-point energies (ZPEs) are also presented together with some other theoretical and experimental results available in the literature in Table V. As the He atoms are located in linear, near T-shape, and antilinear configurations the radial distributions present averaged values at R₀ of 3.82, 3.86, and 5.12 Å, respectively (see Figs. 3 and 4). All complexes are showing high anharmonicity, especially the linear ones, with the ZPEs being more than 60% of their potential well energy.

For the triatomic HeICI molecule we find three different isomers: linear (0,1,0), near T-shape (1,0,0), and antilinear (0,0,1), with binding energies of 18.390, 15.137, and 12.298 cm⁻¹, respectively. These results compare very well to the 2D variational calculations with the ICI distance frozen at its equilibrium value ($r_e = 2.321$ Å), where binding energies of 18.29 cm⁻¹ for the (0,1,0), 15.15 cm⁻¹ for the (1,0,0) and 12.33 cm⁻¹ for the (0,0,1) isomers have been reported.³⁷ In Table V we also include the experimental results based on the HeICI action spectra recorded in the B-X, 3-0 region of the ICI.²⁴ In a series of LIF and action spectroscopy experiments binding energies of 22.0(2) cm⁻¹ have been reported for the linear (0,1,0) isomer, while for the (1,0,0) one values of 19.5(6) and 16.6(3) cm⁻¹ have been estimated based on a thermodynamical model and from recent more direct experimental measurements, respectively.^{24,47,48} The difference between the two isomers from the above experimental studies has been predicted to be 2.5(6) and 5.4 cm⁻¹, respectively, with the present theoretical being 3.25 cm⁻¹. We should point out here that, as we show in Table II, the differences between the most accurate CBS[TQ5] results and employed PES energies count for no more than 2.0 cm⁻¹ at the well-depths values, which depending on the anharmonicity might affect to the binding D₀ energies of the HeICI isomers. One can see

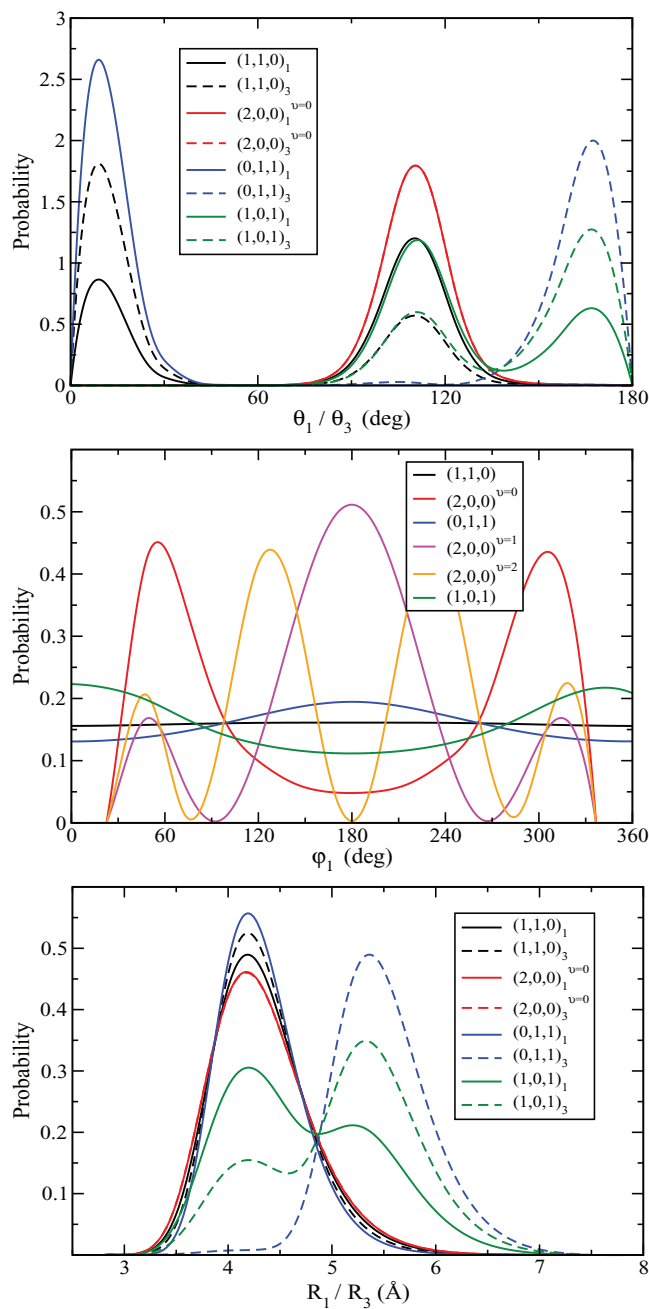


FIG. 3. Angular and radial probability density distributions of the indicated He_2ICl conformers, respectively. The set of coordinates used to describe the He_2ICl complex is $(r, R_1, R_3, \theta_1, \theta_3, \varphi_1)$ (see Fig. 1). In the top and bottom panels we add a subindex to the legends indicating if we are considering the He_1 (solid lines) or the He_3 (dashed lines). In the top panel, we plot the distributions in $\theta_{1,3}$, in the central panel in φ_1 and in the bottom panel in $R_{1,3}$. In the central panel we include two states corresponding to excitations of the φ_1 mode in the $(2,0,0)$ conformer.

that by improving the *ab initio* computations a better agreement could be achieved with the experimental values. Especially, for the $(1,0,0)$ isomer, where the theoretical value is lower by only 1.5 cm^{-1} , although this is not the case for the linear $(0,1,0)$ where larger difference of 3.6 cm^{-1} is found. Moreover, we should note that these differences will have also an effect for the larger clusters due to the additivity of the triatomic potential terms (see Eq. (2)).

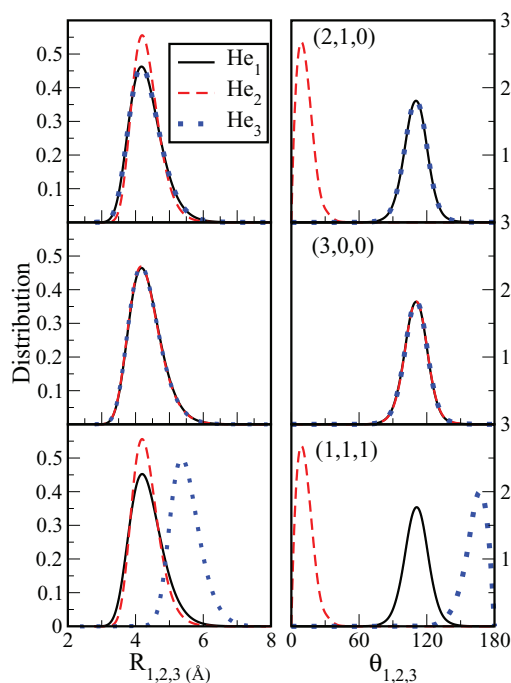


FIG. 4. Probability density distributions in R_1 (black/solid), R_2 (red/dashed), and R_3 (blue/points) in angstroms (left side panels) and in θ_1 (black/solid), θ_2 (red/dashed), and θ_3 (blue/points) in degrees (rightside panels) of the He_3ICl $(2,1,0)$, $(3,0,0)$, and $(1,1,1)$ conformers in the top, central, and bottom panels, respectively.

We should also comment on the theoretical prediction of an antilinear $(0,0,1)$ conformer for HeICl cluster as the transitions corresponding to such conformer have not been detected by the experiment.²² Previous studies carried out on the X and B state of homonuclear dihalogen systems plus a helium atom using high-level *ab initio* methodology have found important differences in the topology of the X and B potential energy surfaces, being the most notable difference the lost of the linear isomer in the B state.^{13,14} Taking into account the Frank-Condon factors for those systems one can see that the transitions between the T-shaped levels are strongly favored over the transitions from the linear conformer in the X ground electronic level to some excited and highly delocalized intermolecular vibrational level in the B electronic excited state. Unfortunately, there is not such a study for a system with a heteronuclear dihalogen molecule. However, due to the differences in the R_0 averaged values mentioned above, it is very likely that the Frank-Condon factors for the transition between the antilinear isomer and the complex in the B state make this transition very unfavorable. In addition to this effect, the differences in binding energy between the different isomers in the X electronic state indicates that, as higher values of the temperature are needed to populate the $(0,0,1)$ conformer, the population of the rotationally excited states of the T-shaped isomers increases and the analysis and assignment of the spectra becomes much more complicated. Apart from the low intensities for such transitions, an additional difficulty for the experiment might come from the presence of transitions involving isotopic species, $\text{He-}^{37}\text{Cl}$, that could hide the ones corresponding to the $(0,0,1)$ isomer.

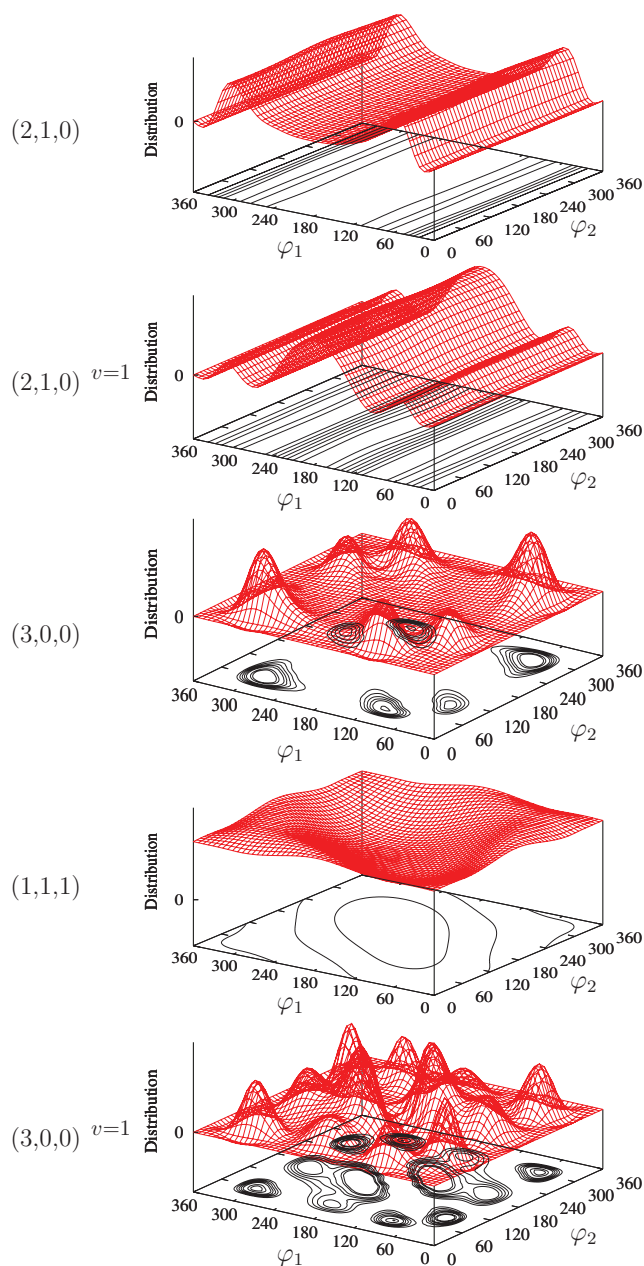


FIG. 5. Two dimensional angular density distributions in φ_1 and φ_2 in degrees of the He₃ICI (2,1,0), (2,1,0)^{v=1}, (3,0,0), (1,1,1), and (3,0,0)^{v=1} states.

In the tetra-atomic case the five lowest bound states, corresponding to the relaxed $v = 0$ (1,1,0), (0,1,1), (2,0,0) isomers and to two vibrationally excited states of the (2,0,0) isomer in the He–He bond, denoted as (2,0,0)^{v=1} and (2,0,0)^{v=2}, have been calculated. The results presented in Table V, where we can see that the 5D and 6D values of the vibrational states are very close in energy, with a maximum difference of 0.1 cm⁻¹ for the (2,0,0) state, indicating the small influence of the r -coordinate in the calculation of states. The 6D MCTDH binding energies of the states are 33.692, 30.883, 30.820, and 28.167 cm⁻¹ for the relaxed (1,1,0), (0,1,1), (2,0,0), and (1,0,1) isomers, respectively. The vibrationally excited states (2,0,0)^{v=1} and (2,0,0)^{v=2} are located at energies 29.730 and 29.505 cm⁻¹, respectively. Also, we found somehow larger differences of 0.78 cm⁻¹ for the (0,1,1) state between the

5D variational and MCTDH results. This was not the case for the He₂Br₂ system, where these differences count less than 0.1 cm⁻¹.³⁴ By carrying out further test calculations we attribute these differences to the better convergence of the present MCTDH computations as compared to the previous variational ones.²⁵ Changing the homonuclear Br₂ to the heteronuclear ICl reduces the symmetry of the system causing the calculations to be computationally much more expensive and the MCTDH method is capable of treating these high dimensionally systems without the computational difficulties found in the variational calculations.

In Fig. 3 we plot the radial and angular distributions of these states. In the top and bottom panels of the distributions probabilities in θ_1/θ_3 and R_1/R_3 (see the coordinate notation of Fig. 1) allow the assignment to the (1,1,0), (0,1,1), (2,0,0), and (1,0,1) isomers. In the central panel of Fig. 3 the distribution probabilities in φ_1 are presented. We include in this panel the distribution probabilities of the (2,0,0)^{v=1} and (2,0,0)^{v=2} states that allow their assignment to excitations of the v He–He stretching mode. The experimental values of the binding energy of the tetra-atomic complexes, 38.6(4) and 33.2(4) for the (1,1,0) and (2,0,0) conformers, have been estimated from the sum of the experimental binding energies of the triatomic complexes,²² therefore, we obtained the expected differences with the calculated theoretical values. However, the energetic order of the calculated isomers at T = 0 K agrees with the temperature dependent experimental results of Boucher *et al.*²² for T = 1.07 and 2.34 K. The lack of the (0,1,1) isomer in the experimental measurements appears also to be a consequence of the possible difficulties of the experiment, discussed above in the case of the (0,0,1) configuration of the triatomic system.

For the He₃ICI molecule, the 9D MCTDH calculations presented here reveal three different possible isomeric structures corresponding to the (2,1,0), (3,0,0), and (1,1,1) configurations at energies 49.599, 47.273, and 46.838 cm⁻¹, respectively (see Table V). In Fig. 4 we present the radial (see left panels) and angular (see right ones) probability density distributions of these states. We also obtained the vibrationally excited states, (2,1,0)^{v=1} and (3,0,0)^{v=1}, with binding energies 48.418 and 45.728 cm⁻¹. In Fig. 5 we show the two dimensional distributions in φ_1 and φ_2 . We can see that, for the (2,1,0)^{v=1} state, the excitation corresponds to φ_1 , the angle between the two He atoms located in the near T-shape well. In the case of the (3,0,0)^{v=1} a much more complicated distribution (see Fig. 5) is found, corresponding to a combined excitation in φ_1 and φ_2 involving the three atoms in the near T-shape well.

In the spectroscopic studies of Boucher *et al.*²² two conformers of the He₃ICI complex have been stabilized, and the corresponding features have been assigned to the (2,1,0) and (3,0,0) configurations, while no evidence of the (1,1,1) configuration has been detected. However, binding energy values or relative stability studies to determine which configuration is more favorable have not been reported in the above experimental study. Thus, we can only see that our theoretical results are in qualitative agreement with the experimental ones, and provide information about the stability of the different conformers, not yet accessible by the experiment.

III. CONCLUSIONS

This manuscript presents theoretical results on the weakly bound vdW He_{2,3}ICl clusters. Two key computational and methodological advantages have enabled us to do this. First, the *ab initio* electronic structure technology that permits to carry out high level calculations for very weak long range intermolecular interactions for systems containing heavy atoms, such as the iodine, and the reliability of the representation of the underlying potential energy surface for such complexes. Second, the availability of performing full dimensional quantum calculations within the MCTDH framework, that allows the treatment of more degrees of freedom than other quantum methods, maintaining the correlation between them. In our theoretical approach the PESs are based on the sum of triatomic HeICl CCSD(T) parameterized potentials plus the He–He interactions. To represent the PESs in a computationally adequate way for the MCTDH calculations natural potential fits are employed. A mode combination scheme was also introduced in order to speed up the improved relaxation computations. In this way various low-lying vibrational states of the He_{2,3}ICl clusters are calculated, and vibrationally averaged structures, ZPEs and binding energies of different isomers, corresponding to (#T,#L,#A) configurations, were obtained. The MCTDH results are compared with previous theoretical data for the 5D tetra-atomic system, and with recent experimental data available for both tetra- and penta-atomic clusters. In particular, for the He₂ICl we obtained the same relative stability as predicted by the experiment for the (1,1,0) and (2,0,0) conformers, while other isomers not detected by the experiment involving a He atom at the antilinear position, the (0,1,1) and (1,0,1) ones were characterized. For the He₃ICl we obtained a qualitative agreement with the experimental observations, since only two isomers, the (2,1,0) and (3,0,0), have been experimentally identified without any values reported on their binding energies. Again a new conformer associated with the antilinear configuration, the (1,1,1) one, is localized, and the difficulties of the experiment to detect such structures for the He_{1,2,3}ICl complexes are analyzed and discussed. However, in order to complement our findings we think that further theoretical investigations, especially on the topology of involved excited electronic states of rare-gas-heteronuclear dihalogen complexes and spectral simulations, are needed together with experimental studies providing additional insights into the interactions of such systems.

ACKNOWLEDGMENTS

The authors thank to Centro de Calculo (IFF), CTI (CSIC), and CESGA for allocation of computer time. This work has been supported by DGICYT, Spain, Grant No. FIS2010-18132 and the COST Action CM1002 (CODECS).

- ¹R. E. Smalley, L. Wharton, and D. H. Levy, *J. Chem. Phys.* **68**, 671 (1978).
- ²J. A. Blazy, B. M. DeKoven, T. D. Russell, and D. H. Levy, *J. Chem. Phys.* **72**, 2439 (1980).
- ³M. Gutmann, D. M. Willberg, and A. H. Zewail, *J. Chem. Phys.* **97**, 8048 (1992).
- ⁴K. Higgins, F.-M. Tao, and W. Klemperer, *J. Chem. Phys.* **109**, 3048 (1998).
- ⁵B. A. Swartz, D. E. Brinza, C. M. Western, and K. C. Janda, *J. Phys. Chem.* **88**, 6272 (1984).

- ⁶J. C. Drobits and M. I. Lester, *J. Chem. Phys.* **86**, 1662 (1987).
- ⁷A. Rohrbacher, N. Halberstadt, and K. C. Janda, *Ann. Rev. Phys. Chem.* **51**, (2000).
- ⁸J. M. Pio, W. E. van der Veer, C. R. Bieler, and K. C. Janda, *J. Chem. Phys.* **128**, 134311 (2008).
- ⁹D. S. Boucher and R. A. Loomis, *Stabilization of Different Conformers of Weakly Bound Complexes to Access Varying Excited-State Intermolecular Dynamics* (Wiley, New York, 2008), pp. 375–419.
- ¹⁰S. M. Cybulski and J. S. Holt, *J. Chem. Phys.* **110**, 7745 (1999).
- ¹¹R. Prosimiti, P. Villarreal, and G. Delgado-Barrio, *Chem. Phys. Lett.* **359**, 473 (2002).
- ¹²Á. Valdés, R. Prosimiti, P. Villarreal, and G. Delgado-Barrio, *Chem. Phys. Lett.* **375**, 328 (2003).
- ¹³Á. Valdés, R. Prosimiti, P. Villarreal, G. Delgado-Barrio, and H.-J. Werner, *J. Chem. Phys.* **126**, 204301 (2007).
- ¹⁴L. Garcia-Gutierrez, L. Delgado-Tellez, Á. Valdés, R. Prosimiti, P. Villarreal, and G. Delgado-Barrio, *J. Phys. Chem. A* **113**, 5754 (2009).
- ¹⁵L. Delgado-Tellez, Á. Valdés, R. Prosimiti, P. Villarreal, and G. Delgado-Barrio, *J. Chem. Phys.* **134**, 214304 (2011).
- ¹⁶P. Villarreal, O. Roncero, and G. Delgado-Barrio, *J. Chem. Phys.* **101**, 2217 (1994).
- ¹⁷C. Meier and U. Manthe, *J. Chem. Phys.* **115**, 5477 (2001).
- ¹⁸A. A. Buchachenko, R. Prosimiti, C. Cunha, G. Delgado-Barrio, and P. Villarreal, *J. Chem. Phys.* **117**, 6117 (2002).
- ¹⁹R. Prosimiti, C. Cunha, A. A. Buchachenko, G. Delgado-Barrio, and P. Villarreal, *J. Chem. Phys.* **117**, 10019 (2002).
- ²⁰Á. Valdés, R. Prosimiti, P. Villarreal, G. Delgado-Barrio, D. Lemoine, and B. Lepetit, *J. Chem. Phys.* **126**, 244314 (2007).
- ²¹Á. Valdés, R. Prosimiti, P. Villarreal, and G. Delgado-Barrio, *J. Chem. Phys.* **122**, 044305 (2005).
- ²²D. S. Boucher, J. P. Darr, D. B. Strasfeld, and R. A. Loomis, *J. Phys. Chem. A* **112**, 13393 (2008).
- ²³A. Jäckle and H.-D. Meyer, *J. Chem. Phys.* **109**, 3772 (1998).
- ²⁴J. P. Darr and R. A. Loomis, *J. Chem. Phys.* **129**, 144306 (2008).
- ²⁵Á. Valdés, R. Prosimiti, P. Villarreal, and G. Delgado-Barrio, *J. Chem. Phys.* **125**, 014313 (2006).
- ²⁶C. Diez-Pardos, Á. Valdés, R. Prosimiti, P. Villarreal, and G. Delgado-Barrio, *Theor. Chem. Acc.* **118**, 511 (2007).
- ²⁷Á. Valdés, P. Barragán, R. Pérez de Tudela, L. Delgado-Tellez, J. S. Medina, and R. Prosimiti, “A theoretical characterization of multiple isomers of the He₂I₂ complex,” *Chem. Phys.* (submitted).
- ²⁸D. López-Durán, M. P. de Lara-Castells, G. Delgado-Barrio, P. Villarreal, C. Di. Paola, F. A. Gianturco, and J. Jellinek, *J. Chem. Phys.* **121**, 2975 (2004).
- ²⁹M. P. de Lara-Castells, D. López-Durán, G. Delgado-Barrio, P. Villarreal, C. Di Paola, F. A. Gianturco, and J. Jellinek, *Phys. Rev. A* **71**, 033203 (2005).
- ³⁰P. M. Felker, *J. Chem. Phys.* **125**, 184313 (2006).
- ³¹M. P. de Lara-Castells, R. Prosimiti, G. Delgado-Barrio, D. López-Durán, P. Villarreal, F. A. Gianturco, and J. Jellinek, *Phys. Rev. A* **74**, 053201 (2006).
- ³²H.-D. Meyer, U. Manthe, and L. S. Cederbaum, *Chem. Phys. Lett.* **165**, 73 (1990).
- ³³M. H. Beck, A. Jäckle, G. A. Worth, and H.-D. Meyer, *Phys. Rep.* **324**, 1 (2000).
- ³⁴Á. Valdés, R. Prosimiti, P. Villarreal, and G. Delgado-Barrio, *J. Chem. Phys.* **135**, 054303 (2011).
- ³⁵R. A. Aziz and M. J. Slaman, *J. Chem. Phys.* **94**, 8047 (1991).
- ³⁶See supplementary material at <http://dx.doi.org/10.1063/1.3671611> for the computed CCSD(T) interaction energies for ICl and fitting coefficients of HeICl.
- ³⁷R. Prosimiti, C. Cunha, P. Villarreal, and G. Delgado-Barrio, *J. Chem. Phys.* **117**, 7017 (2002).
- ³⁸M. J. Frisch, G. W. Trucks, and H. B. Schlegel *et al.*, GAUSSIAN 09 Revision A.1, Gaussian, Inc., Wallingford, CT, 2009.
- ³⁹H.-J. Werner, P. J. Knowles, R. Lindh, F. R. Manby, M. Schütz *et al.*, MOLPRO, version 2009.1, a package of *ab initio* programs, 2009.
- ⁴⁰M. Dolg, *Habilitationschrift* (Universität Stuttgart, 1997).
- ⁴¹J. M. L. Martin and A. Sundermann, *J. Chem. Phys.* **114**, 3408 (2001).
- ⁴²K. A. Peterson, D. Figgen, E. Goll, H. Stoll, and M. Dolg, *J. Chem. Phys.* **119**, 11113 (2003).
- ⁴³R. A. Kendall, T. H. Dunning, and R. J. Harrison, *J. Chem. Phys.* **96**, 6796 (1992).

- ⁴⁴K. A. Peterson, D. E. Woon, and T. H. Dunning, *J. Chem. Phys.* **100**, 7410 (1994).
- ⁴⁵G. A. Worth, M. H. Beck, A. Jäckle, and H.-D. Meyer, The MCTDH package, Version 8.2 (2000); H.-D. Meyer, Version 8.3 (2002), Version 8.4 (2007); See <http://mctdh.uni-hd.de>.
- ⁴⁶A. Jäckle and H.-D. Meyer, *J. Chem. Phys.* **104**, 7974 (1996).
- ⁴⁷D. S. Boucher, J. P. Darr, M. D. Bradke, R. A. Loomis, and A. B. McCoy, *Phys. Chem. Chem. Phys.* **6**, 5275 (2004).
- ⁴⁸J. P. Darr, R. A. Loomis, and A. B. McCoy, *J. Chem. Phys.* **122**, 044318 (2005).